

The supporting information

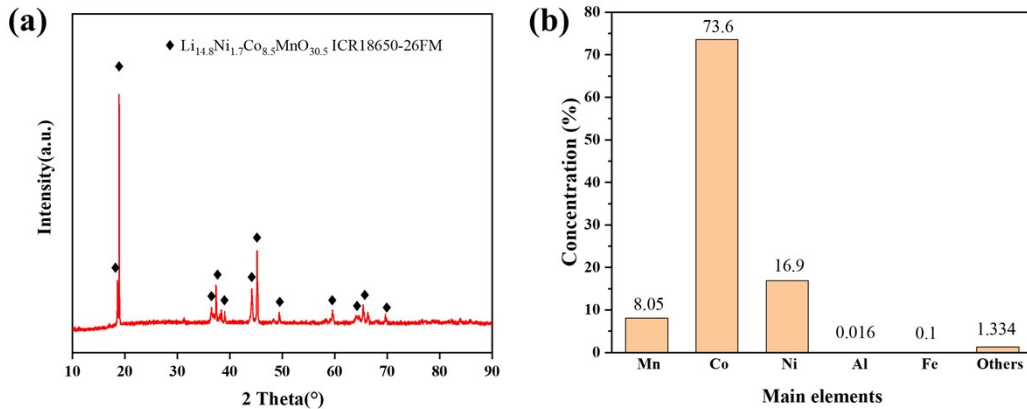


Fig. S1 (a) XRD and (b) XRF images of spent LIBs.

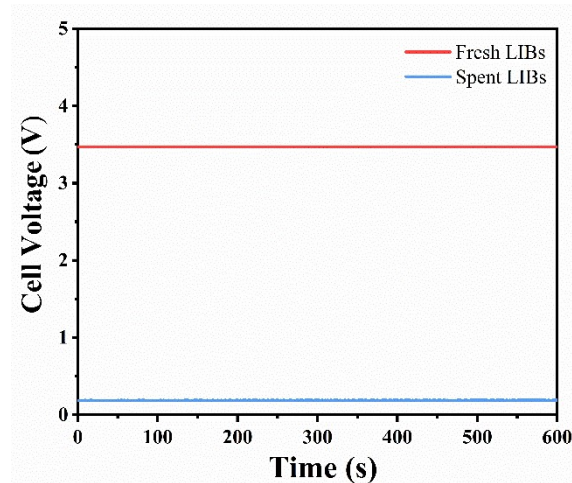


Fig. S2 Open-circuit voltage of spent lithium-ion batteries after discharge

Table S1 Recovery ratios (%) of the major elements by calculations

Element	Mn	Co	Ni
Recovery ratios (%)	73.52	87.38	92.21

The supporting information

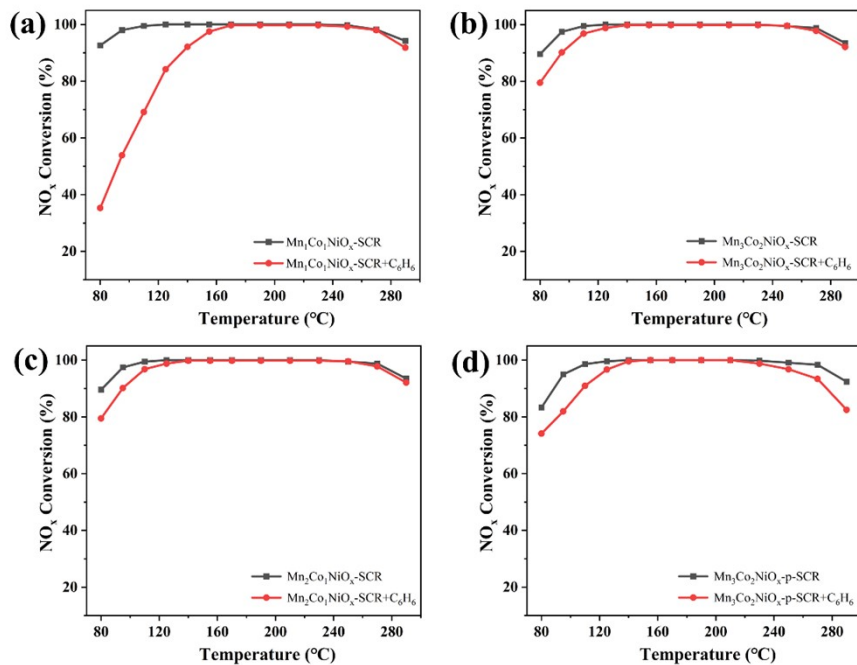


Fig.S3. (a) NO_x conversion of catalysts with different manganese contents in different atmospheres (a) MnCo₂NiO_x; (b) Mn₁Co₁NiO_x; (c) Mn₃Co₂NiO_x ; (d) Mn₃Co₂NiO_x-p

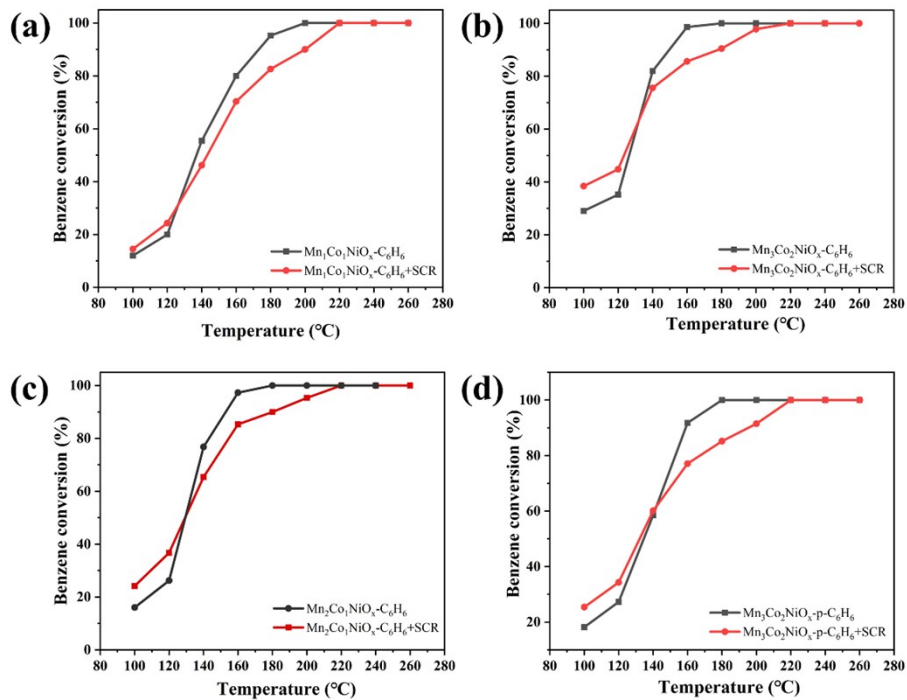


Fig.S4. (a) Benzene conversion of catalysts with different manganese contents in different atmospheres (a) MnCo₂NiO_x; (b) Mn₁Co₁NiO_x; (c) Mn₃Co₂NiO_x ; (d) Mn₃Co₂NiO_x-p

The supporting information

Table S2 Different crystallite parameters of $\text{Mn}_3\text{Co}_2\text{NiO}_x$ and $\text{Mn}_3\text{Co}_2\text{NiO}_x\text{-p}$ by XRD results.

Sample	(3 1 1) plane		
	2 theta($^{\circ}$)	FWHM($^{\circ}$)	D (nm)
$\text{Mn}_3\text{Co}_2\text{NiO}_x$	36.3	0.694	14.8
$\text{Mn}_3\text{Co}_2\text{NiO}_x\text{-p}$	36.28	0.658	15.6

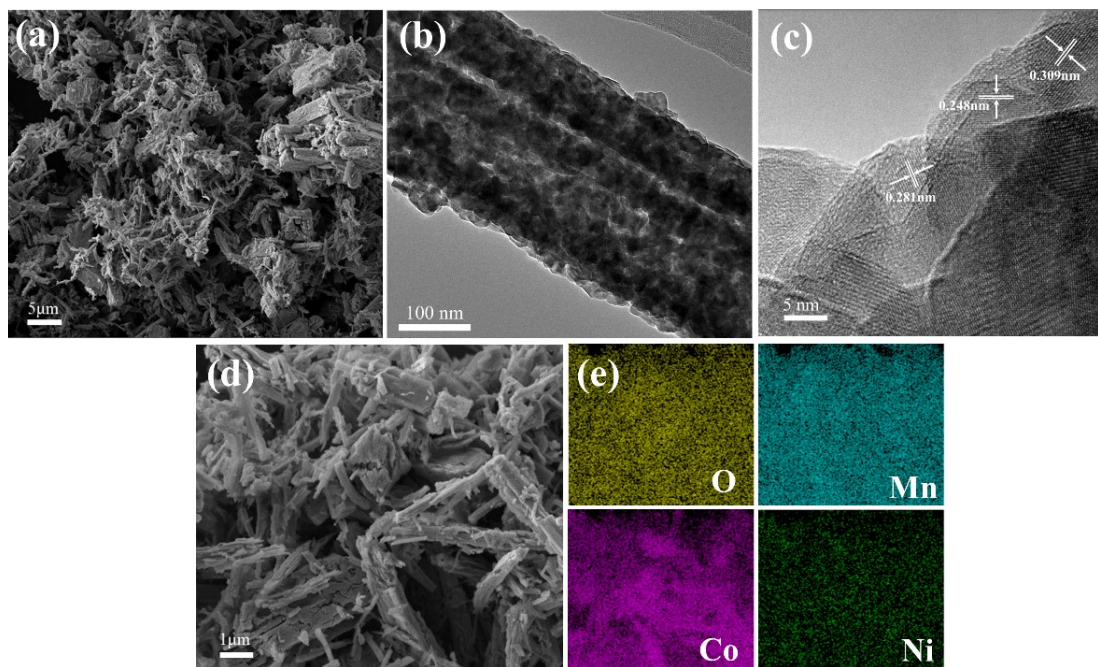


Fig. S5 SEM images of $\text{Mn}_3\text{Co}_2\text{NiO}_x\text{-MS}$ catalyst at (a) 5 μm and (d) 1 μm ; (b-c) HR-TEM images; (e-f) EDS elemental mapping of $\text{Mn}_3\text{Co}_2\text{NiO}_x\text{-MS}$ catalyst

The supporting information

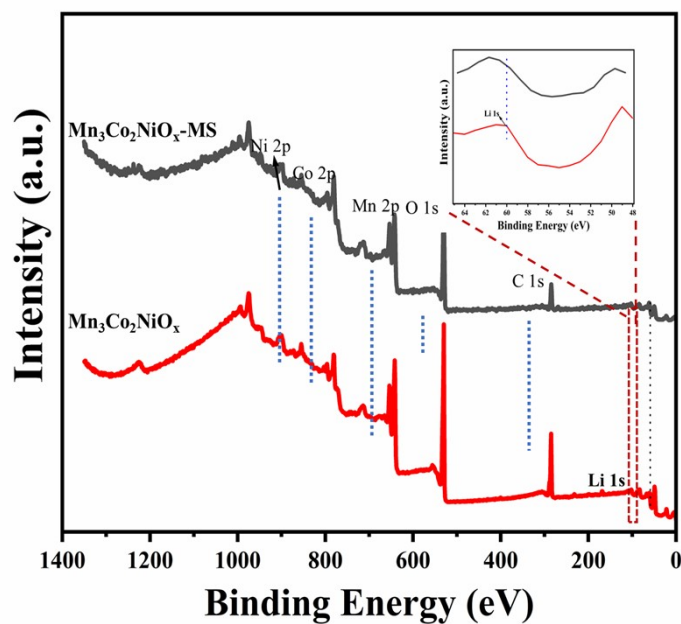


Fig. S6 XPS survey spectra of $\text{Mn}_3\text{Co}_2\text{NiO}_x$ and $\text{Mn}_3\text{Co}_2\text{NiO}_x$ -MS

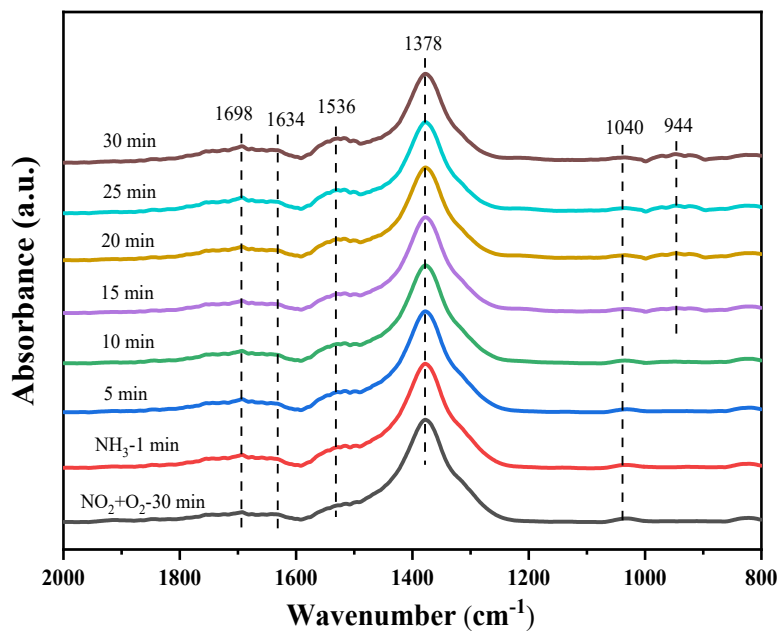


Fig. S7. In situ DRIFTS of $\text{Mn}_3\text{Co}_2\text{NiO}_x$ catalysts with NH_3 after pre-adsorption of $\text{NO} + \text{O}_2$ for different times at 190°C

The supporting information

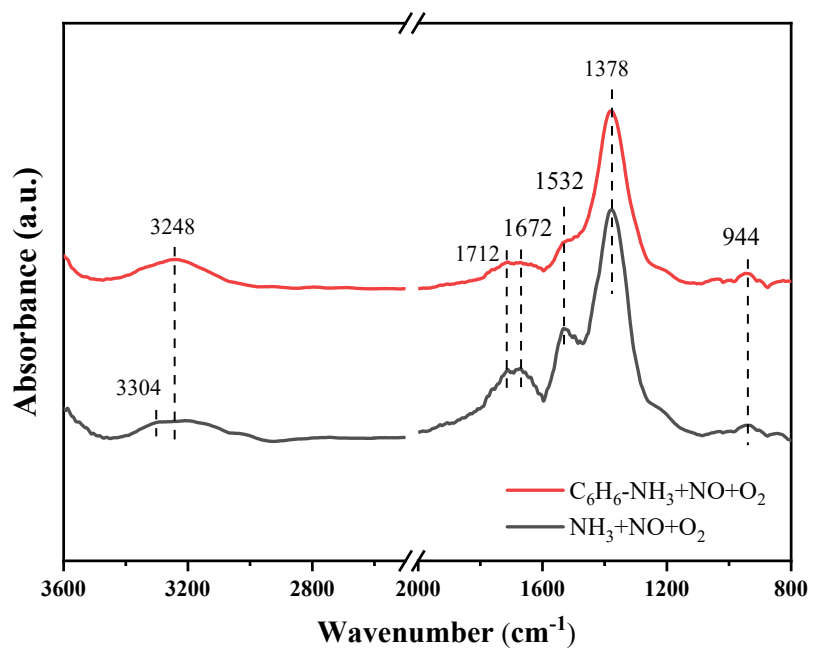


Fig S8 In situ DRIFTS spectra of $\text{Mn}_3\text{Co}_2\text{NiO}_x$ catalysts after reaction with SCR gases in the presence or absence of benzene at 190°C